Nuclear Instruments and Methods in Physics Research B 286 (2012) 218–222

Contents lists available at SciVerse ScienceDirect

Nuclear Instruments and Methods in Physics Research B

journal homepage: www.elsevier.com/locate/nimb

# Microstructural evolution of the pyrochlore compound $Er_2Ti_2O_7$ induced by light ion irradiations

Y.H. Li [a,b,*], Y.Q. Wang [b], C.P. Xu [a], J.A. Valdez [b], M. Tang [b], K.E. Sickafus [b]

[a] *School of Nuclear Science and Technology, Lanzhou University, Lanzhou 730000, China*
[b] *Materials Science & Technology Division, Los Alamos National Laboratory, Los Alamos, NM 87545, USA*

ARTICLE INFO

*Article history:*
Received 30 August 2011
Received in revised form 12 September 2011
Available online 30 December 2011

*Keywords:*
$Er_2Ti_2O_7$
Ion irradiation
GIXRD
Swelling effects

ABSTRACT

In this report, we present results of an irradiation damage study on a pyrochlore compound, $Er_2Ti_2O_7$. Polycrystalline $Er_2Ti_2O_7$ was irradiated with 400 keV $Ne^{2+}$ ions at cryogenic temperature (~77 K) to fluences ranging from $2 \times 10^{18}$ to $2 \times 10^{19}$ ions/m$^2$. Irradiation-induced microstructural evolution was examined using grazing incidence X-ray diffraction (GIXRD) at angles of $\gamma = 0.25°$ and 3°. It was found that the irradiated $Er_2Ti_2O_7$ undergoes significant lattice swelling before succumbing to a radiation-induced partial amorphization transformation. Both of the extent of the lattice swelling and the lattice disorder of the $Er_2Ti_2O_7$ increase with increasing Ne ion fluence prior to partial amorphization. We present here a detailed discussion regarding the nature of the defects responsible for the observed lattice swelling and disorder in $Er_2Ti_2O_7$.

## 1. Introduction

Pyrochlores $A_2B_2O_7$ belong to $Fd\bar{3}m$ space group, and is a superstructure of the fluorite structure ($MO_2$), but with two cations and one eighth of the oxygen anion absent, as shown in Fig. 1. The larger $A^{3+}$ cation at 16d is eight-coordinated and located within a distorted cubic coordination polyhedron. The smaller $B^{4+}$ cation at 16c is six-coordinated and in a distorted octahedron. There are two unique oxygen sites: the 48f oxygen is coordinated to two $B^{4+}$ cations and two $A^{3+}$ cations, while the 8b oxygen is in tetrahedral coordination with only $A^{3+}$ cations. An unoccupied interstitial site at 8a is surrounded by four $B^{4+}$ ions, and the "vacancies" at the 8a site are ordered on the anion sublattice. The oxygen at the 48f site is slightly displaced from that in the ideal fluorite structure ($x_{48f} = 0.3750$) toward the 16d site cation. The magnitude of the displacement is measured by the value of the positional parameter, $x_{48f}$. Because all the atoms except for the 48f oxygen are on special positions, the pyrochlore structure can be completely described by the cubic lattice parameter, *a*, and the 48f oxygen positional parameter, *x*. For $x = 0.3750$, the 16c site coordination polyhedron is regular cube, and the 16d site polyhedron is distorted to a trigonally flattened octahedron [1].

Pyrochlores $A_2B_2O_7$ are of important candidate ceramic waste forms for actinide immobilization and are among the principal host phases currently considered for the disposition of Pu from dismantled nuclear weapons and the "minor" actinides (e.g., Np, Am, Cm) generated by the nuclear fuel cycle [2,3]. Since the resulting nuclear waste form will be subjected to alpha-decay events, the structure of pyrochlore waste forms are naturally subject to irradiation induced damage as a result of the accumulation of defects (e.g., the formation of anti-site defects, Frenkel pairs, etc.). The irradiation induced microstructural changes include amorphization, volume expansion, cracking, and reduced chemical durability of the waste form. Thus, it is very important to study damage accumulation and amorphization process in the related waste form materials.

Numerous experimental studies have been carried out to study the radiation-induced phase transformation from order-to-disorder and crystalline to amorphous structure [4–16]. More specifically, great efforts have been focused on identifying factors that influence the response of pyrochlore to ion irradiation-induced amorphization. For example, Lian et al. have carried out extensive studies on the radiation-induced amorphization of rare-earth pyrochlores using in situ transmission electron microscope technique [4–9]. These studies suggest that an ion beam-induced pyrochlore-to-fluorite (order-to-disorder) structural transition occurs in all the irradiated pyrochlore compositions. They further concluded that upon ion irradiation of these pyrochlore compositions, the cation and anion disordering processes occur independently, and the anion disordering precedes the cation disordering [17]. In other words, these in situ TEM studies found that a pyrochlore structure with significantly ordered cations and completely disordered anions is formed upon ion irradiation, prior to the observed phase transition from an ordered pyrochlore to an amorphous structure. However, the

---

[*] Corresponding author at: School of Nuclear Science and Technology, Lanzhou University, Lanzhou 730000, China.

*E-mail address:* liyuhong@lzu.edu.cn (Y.H. Li).

0168-583X/$ - see front matter © 2011 Elsevier B.V. All rights reserved.
doi:10.1016/j.nimb.2011.12.034

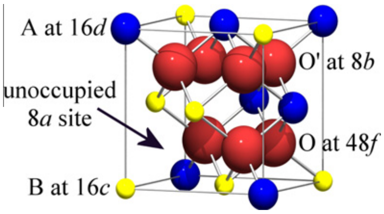

**Fig. 1.** The structure of pyrochlore $A_2B_2O_7$.

first-principles calculations performed by Lian et al. [5] on the defect formation energies of $Y_2(Ti, Sn, Ar)_2O_7$ pyrochlore compounds indicated that cation antisite disordering precedes oxygen anion disordering in these pyrochlore structures, inconsistent with the in situ TEM experimental conclusions. The purpose of the study presented here is to investigate the microstructural evolution of pyrochlore $Er_2Ti_2O_7$ upon 400 keV $Ne^{2+}$ ion irradiation at cryogenic temperature (~77 K) by using X-ray diffraction measurement and simulation tools.

## 2. Experimental procedure

Polycrystalline $Er_2Ti_2O_7$ samples were synthesized from $Er_2O_3$ (Alfa Aesar, 99.99% purity), and $TiO_2$ powers (Aldrich Chemical company, 99.99% purity), by conventional ceramic processing procedures. The measured densities of the sintered pellets were larger than ~90% of theoretically density.

Ion irradiations were performed under cryogenic condition ($T_{\text{substrate}} \sim 77$ K) at the Ion Beam Materials Laboratory, Los Alamos National Laboratory, using a 200 kV Danfysik high current research ion implanter. The 400 keV $Ne^{2+}$ ions were implanted at normal incidence at fluencies ranging from $2 \times 10^{18}$ to $2 \times 10^{19}$ ions/m$^2$ using an ion flux of $\sim 1 \times 10^{16}$ ions/m$^2$ s. The projected range of the 400 keV Ne ions in $Er_2Ti_2O_7$ was estimated using the Monte Carlo code SRIM [18]. The projected range, $R_p$, was estimated to be 407 nm (with target density $\rho = 7.039$ g/cm$^3$), with a longitudinal straggling, $\Delta R_p$, of 131 nm. In these calculations, we assumed the threshold displacement energies for Er, Ti, and O are all 40 eV (these energies are arbitrary assumptions because we currently do not have experimental or theoretical estimates for these values).

Grazing incident X-ray diffraction (GIXRD) was used to characterize the crystal structure of pristine and ion irradiated samples using a Bruker AXS D8 advanced X-ray diffractometer, $\theta$–$2\theta$ geometry, Cu-K radiation, and the X-ray angles of incidence ($\gamma$) are 0.25° and 3°. The depth of the X-rays in $Er_2Ti_2O_7$ for $\gamma = 0.25°$ and 3° grazing incident angles are 66 and 711 nm, respectively. The X-ray penetration depths were estimated by using geometrically method [19]. The step size of the scan angle was 0.008° and a dwell time of 2s per step. The scan range was 10–70°.

XRD simulation calculation was carried out using the Powder Diffraction function in Reflex module included in software Materials Studio. Reflex is a module that can be used not only to study a perfect crystal lattice but also to predict the extent to which a given lattice accommodates point defects [20]. For perfect $Er_2Ti_2O_7$ XRD simulations, we chose the origin at $Er^{3+}$ 16d site, thus the atoms occupy the following special positions: $Er^{3+}$ at 16d (0,0,0), $Ti^{4+}$ at 16c (0.5,0.5,0.5), O at 48f ($x$,0.125,0.125), and O′ at 8b (0.375,0.375,0.375). The defect structures of $Er_2Ti_2O_7$ pyrochlore were simulated based on a large unit cell containing 119 atoms, by assigning $Er^{3+}$ and $Ti^{4+}$ cations at random to the available 16d and 16c sites. A similar procedure was employed on the oxygen sublattice, where the anions were distributed not only to the 48f and 8b sites occupied in pyrochlore but also to the normally unoccupied vacancy 8a site.

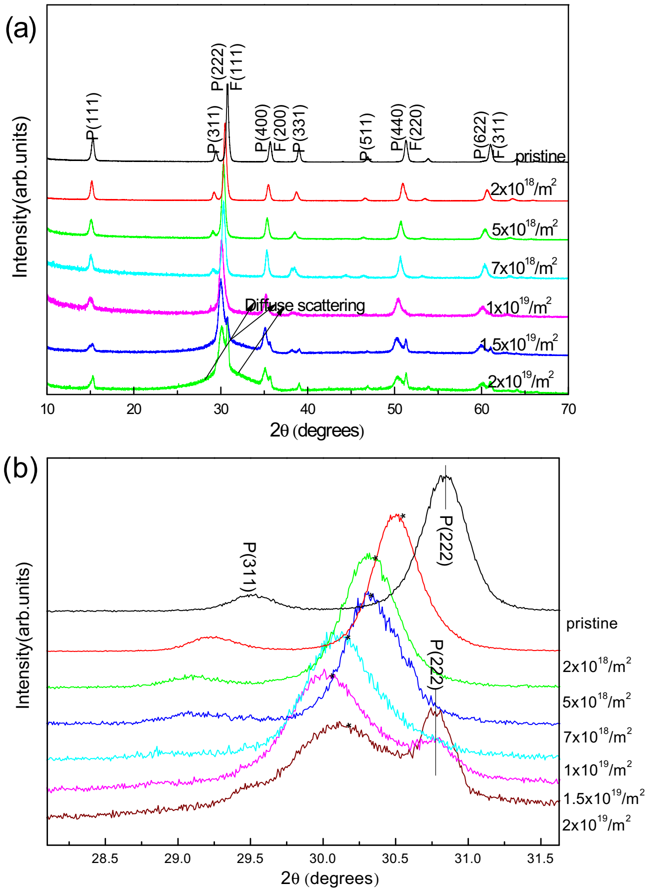

**Fig. 2.** GIXRD patterns obtained from unirradiated and irradiated $Er_2Ti_2O_7$ samples to fluence of $1 \times 10^{18}$–$2 \times 10^{19}$/m$^2$ at X-ray incidence angle of 0.25°. (a) $2\theta = 10$–70°, (b) $2\theta = 28.1$–31.6°.

## 3. Results and discussion

Fig. 2(a) shows GIXRD patterns obtained from pristine $Er_2Ti_2O_7$ and $Er_2Ti_2O_7$ irradiated with 400 keV $Ne^{2+}$ ions at fluences of $2.0 \times 10^{18}$ ions/m$^2$ to $2.0 \times 10^{19}$ ions/m$^2$ at an X-ray incidence angle of 0.25°. The samples exhibit a pyrochlore superlattice structure: diffraction peaks of $P\{111\}$, $P\{311\}$, $P\{331\}$, and $P\{511\}$ are pyrochlore superlattice reflections, while $P\{222\}$, $P\{400\}$, $P\{440\}$, $P\{622\}$, and $P\{444\}$ (or $F\{111\}$, $F\{200\}$, $F\{220\}$, $F\{311\}$, and $F\{222\}$) are fundamental fluorite reflections. From Fig. 2, one can discern the following phenomena: first, all peaks shift towards smaller $2\theta$ with increasing Ne ion fluence from $2 \times 10^{18}$ to $1.5 \times 10^{19}$/m$^2$, and then all peaks move back to larger $2\theta$ as Ne ion fluence reaches to $2 \times 10^{19}$/m$^2$ (see Fig. 2(b), zoom on $2\theta = 28.1$–31.6° region of GIRXD pattern in Fig. 2(a), showing the gradual displacement of $P\{311\}$ and $P\{222\}$ reflections with increasing Ne ion fluence). Second, the irradiated samples became partially amorphous as Ne ion fluence reaches $1.5 \times 10^{19}$/m$^2$ due to a broad diffraction feature occurring at the basis of the $P\{222\}$. Third, the intensity of the pyrochlore superlattice reflections $P\{hkl\}$ ($h,k,l$ are all odd numbers), relative to the intensity of fluorite reflection $P\{h,k,l\}$ ($h,k,l$ are all even numbers), are gradually diminishing with increasing Ne ion fluence. Fourth, a small peak emerges at the right side of each GIXRD pattern as Ne ion fluence reaches to $1.5 \times 10^{19}$/m$^2$.